

Accepted Manuscript

Biodegradable PLGA implants containing doxorubicin-loaded chitosan nanoparticles for treatment of breast tumor-bearing mice

Amirhosein Kefayat, Sedigheh Vaezifar



PII: S0141-8130(19)32456-0
DOI: <https://doi.org/10.1016/j.ijbiomac.2019.06.055>
Reference: BIOMAC 12561
To appear in: *International Journal of Biological Macromolecules*
Received date: 3 April 2019
Revised date: 3 June 2019
Accepted date: 9 June 2019

Please cite this article as: A. Kefayat and S. Vaezifar, Biodegradable PLGA implants containing doxorubicin-loaded chitosan nanoparticles for treatment of breast tumor-bearing mice, *International Journal of Biological Macromolecules*, <https://doi.org/10.1016/j.ijbiomac.2019.06.055>

This is a PDF file of an unedited manuscript that has been accepted for publication. As a service to our customers we are providing this early version of the manuscript. The manuscript will undergo copyediting, typesetting, and review of the resulting proof before it is published in its final form. Please note that during the production process errors may be discovered which could affect the content, and all legal disclaimers that apply to the journal pertain.

Biodegradable PLGA implants containing doxorubicin-loaded chitosan nanoparticles for treatment of breast tumor-bearing mice

Amirhosein Kefayat¹, Sedigheh Vaezifar^{2}*

¹ Department of Oncology, Cancer Prevention Research Center, Isfahan University of Medical Sciences, Isfahan 81746-73461, Iran

² Department of Medical Engineering, Payame Noor University, Isfahan, Iran

** Corresponding author:*

Sedigheh Vaezifar

Department of Medical Engineering, Payame Noor University, Isfahan, Iran.

Tel: +98-3133521803

Fax: +98-3133521802

E-mail: s.vaezifar@pnu.ac.ir

Abstract

Drug-loaded implants have exhibited many advantages over intravenous or oral drug administration, especially for cancer treatment. Therefore, biodegradable implants have received lots of attention for controlled release and delivery of anti-cancer drugs. In the present study, doxorubicin-loaded chitosan (CS-DOX) nanoparticles were synthesized and characterized. Subsequently, polylactic-co-glycolic acid (PLGA) was used as a maintainer to form a biodegradable implant containing CS-DOX nanoparticles for subcutaneous implantation (PLGA/CS-DOX). The therapeutic efficacy of these implants was investigated in different groups of 4T1 breast tumor-bearing BALB/c mice including no-treatment, PLGA, PLGA/CS, PLGA/CS-DOX, and doxorubicin (5 mg/kg/day). The most therapeutic efficacy was observed at PLGA/CS-DOX implants which significantly ($P<0.05$) inhibited breast tumors' growth and metastasis. The PLGA/CS-DOX implant was completely biodegradable and caused 71% and 62 % decrease in the tumors' volume and lung metastatic nodules in comparison with no-treatment, respectively. In addition, 41 days increase in the tumor-bearing mice survival of the PLGA/CS-DOX group was observed in comparison with the no-treatment group. Therefore, the subcutaneous implantation of PLGA/CS-DOX can be an appropriate choice for replacement of multiple-doses injections of doxorubicin for breast cancer treatment.

Keywords: Breast cancer, Subcutaneous implant, PLGA, Chitosan nanoparticles, Doxorubicin, Metastasis.

Abbreviations:

CS: chitosan

DOX: doxorubicin

PLGA: polylactic-co-glycolic acid

CS-DOX: doxorubicin-loaded chitosan

EPR: enhanced permeability and retention

PBS: phosphate buffer solution

SEM: scanning electron microscope

DLS: dynamic light scattering

1. Introduction

Breast cancer is the most common cancer among women. More than one million new cases are diagnosed every year [1, 2]. Metastasis is the main cause of breast cancer patients' mortality [3].

Breast cancer metastasis is characterized by breast cancer cells' migration to the regional lymph nodes, bone marrow, lung, and liver [4]. Despite advance achievements in the breast cancer treatment, the metastatic patients' prognosis is still poor and not satisfying [5].

One of the most common and useful breast cancer chemotherapy drugs is doxorubicin [6]. It has an excellent anti-proliferative and cytotoxic effect on the primary and metastatic breast cancer [7]. Intercalation into DNA, disruption of topoisomerase-II-mediated DNA repair, and generating free radicals which cause cellular damages are the main mechanisms of action for doxorubicin [8]. However, side effects of doxorubicin can significantly decrease the treatment outcomes and limit its utilization. Many studies have focused on the enhancement of doxorubicin therapeutic efficacy by improving tumor-specific drug delivery [9, 10]. Chitosan nanoparticles have been vastly used as promising carriers for passive tumor targeting [11]. Also, it has exhibited high efficiency for sustained drug-release [12]. Loading of chemotherapy drugs in the chitosan nanoparticles not only enhances their therapeutic efficacy in the solid tumors' treatment but also, reduces the side effects [13]. In addition, chitosan nanoparticles can increase the drugs' bioavailability which highly affects the anti-tumor efficacy [14]. Tamoxifen-loaded chitosan

nanoparticles increased the accumulation of tamoxifen in tumor cells through enhancing of the permeability and retention (EPR) effect, induction of caspase-dependent apoptosis, and improving of antitumor activity [12]. In addition, chitosan nanoparticles per se can cause anti-proliferative and pro-apoptotic effects on the cancer cells [15, 16].

Chemotherapy courses are usually long-term which routinely need multiple injections and are highly time consuming which can considerably decrease patients' comfort and compliance [17, 18]. Implants which contain chemotherapy drugs have exhibited many advantages including elimination of daily dosing and injections, maintenance of the steady-state concentration of the drug, better patient's comfort and compliance over intravenous or oral administrations [19-23]. Biodegradable polymers have received lots of attention for developing these implants. Poly(lactic-co-glycolic) acid or PLGA is a completely biodegradable and biocompatible copolymer which has been broadly utilized for this purpose [24, 25]. PLGA exhibits strong physical properties and have been extensively studied as drug delivery vehicle. Also, FDA has approved many PLGA-based devices [26, 27]. Many studies have employed subcutaneous or intratumoral PLGA-based implants for controlled drug release in the long-term periods [28]. PLGA is more useful than the several available biodegradable polymers for implants' formation due to its long history of experimental and clinical trials, promising degradation characteristics, controlled and sustained drug release and delivery performance [29, 30]. Recent studies have demonstrated that degradable PLGA implants can be used for sustained drug release at required doses. Also, it is possible to tune the overall physical properties of the polymer-drug matrix by controlling the relevant parameters to achieve a desired dosage and release interval [31, 32].

In the present study, doxorubicin-loaded chitosan nanoparticles were incorporated into the PLGA based implants (PLGA/CS-DOX). Then, the PLGA/CS-DOX implants were subcutaneously

implanted at 4T1 tumor-bearing BALB/c mice to inhibit breast tumor's growth and metastasis. Chitosan nanoparticles play the role of an anti-proliferative and anti-metastatic carrier for doxorubicin delivery to the breast cancer cells. In addition, PLGA as a biodegradable polymer can prepare an appropriate matrix for incorporation of CS-DOX nanoparticles for sustained release and tumor-specific drug delivery. To the best of our knowledge, this is the first time to employ a subcutaneous implant with this composition for the treatment of breast tumor-bearing mice.

2. Materials and Methods

2.1. Materials

PLGA (LA=GA 85=15; Mw^{1/2}50,000–75,000) and acid soluble chitosan (low molecular weight with a deacetylation degree of >85%) were purchased from Sigma-Aldrich (St. Louis, MO, USA). Sodium tripolyphosphate, acetic acid, and all other reagents were purchased from Merck (Darmstadt, Germany). RPMI 1640 medium, 10% fetal bovine serum (FBS), penicillin, streptomycin was purchased from Sigma, USA. All the cell culture supplies including plates, flasks, pipettes, etc. were purchased from Millipore, USA.

2.2. Preparation of chitosan nanoparticles

Low molecular weight chitosan (Sigma Aldrich, Germany) was dissolved in acetic acid 1% (w/v). The pH of the solutions was raised to 4.6–4.8 by addition of the appropriate amount of NaOH. Aqueous sodium tripolyphosphate (TPP) solutions were prepared by dissolving TPP in distilled water. The TPP solution was then added drop-wise to a chitosan solution while stirred with a magnetic stirrer (IKA, Basic 2, Germany) at room temperature to form chitosan nanoparticles spontaneously. Turbidity point was determined by laser flash pointer. The mixture was then stirred during the reaction time. The temperature of reaction and pH were kept constant.

The chitosan concentration and TPP concentration were 1.0 mg/ml, and reaction time was 60 min. Subsequently, the nanoparticle suspension was centrifuged at 20,000 rpm for 10 min. The chitosan nanoparticles were extensively washed with distilled water to remove any impurity. Finally, the nanoparticles were precipitated and dried at 70 °C for 24 h. The chitosan nanoparticles synthesis was performed in the specific conditions using high shear and low speed mixing systems. The agglomerated chitosan nanoparticles were deagglomerated by ultrafine milling process. In addition, the percentage yields of chitosan nanoparticles were calculated from the weight of dried nanoparticles recovered and sum of initial dry weight of starting material [33] as the following equilibrium:

$$\text{Yield (\%)} = \frac{W_{CSNP}}{W_{CS}} \times 100 \quad (1)$$

where W_{CSNP} = the total weight of the prepared chitosan nanoparticles (mg), W_{CS} = the total weight of the initial chitosan (mg).

2.3. Doxorubicin-loaded chitosan nanoparticles preparation

Doxorubicin-loaded chitosan (CS-Dox) nanoparticles were prepared by adding an aqueous solution of doxorubicin hydrochloride (1 mg/mL) into the chitosan nanoparticles suspension (containing 20 mg of nanoparticles). The encapsulation of Dox in CS nanoparticles was achieved by continuous stirring of the suspension mixture in the dark overnight at room temperature. The CS-DOX nanoparticles were separated by centrifugation at 25°C, 10,000 rpm for 1 hour. Remaining free doxorubicin in the supernatant was measured for its absorbance at $\lambda = 485$ nm by using UV-Vis Spectrophotometer (PerkinElmer Lambda 35, Perkin Elmer, Boston, MA, USA). CS-Dox nanoparticles were washed and centrifuged 3 times, and then oven dried overnight at 55 °C (FD 115, Fisher Scientific, Limburg, Germany).

2.4. Implantable device fabrication

The microspheres of Poly (lactide-co-glycolide) (PLGA) were prepared by emulsifying a 6% solution of PLGA (LA/GA 85/15; Mw=50,000–75,000) in dichloromethane in 1% poly (vinyl alcohol) (PVA). Microspheres were washed four times with deionized water to remove residual PVA and lyophilized overnight. The PLGA microspheres' morphology was observed using a scanning electron microscope (Seron Technology AIS 2500, India). The diameters of the resulting microsphere were determined using the Image J software from the SEM micrographs. The measured values were averaged.

At the next step, PLGA microspheres and CS-Dox were mixed and the mixture was pressed in a steel die at 1500 psi (5 mm diameter, 2 mm height). The ingredient of the implants is as follow: PLGA (PLGA 100%), PLGA/CS (PLGA:CS = 50%:50%), PLGA/CS-Dox (PLGA:CS:Dox = 45:45:10)

2.5. Drug loading content and encapsulation efficiency

The drug loading and encapsulation efficiency in the chitosan nanoparticles were analyzed by calculating the difference between the total of the drug fed (W_t) and the free drug (W_f) concentrations in the nanoparticles supernatant per weight of chitosan nanoparticles. Data were given as average measurements of three independent values. Drug loading and encapsulation efficiency are calculated by equations (2) and (3) below according to previous studies [8]:

$$\text{Loading content} = \frac{W_t - W_f}{W_{np}} \times 100 \quad (2)$$

where W_t = the total weight of drug fed, W_f = the weight of the non-encapsulated free drug, W_{np} = the weight of the nanoparticles.

$$\text{Encapsulation efficiency} = \frac{W_t - W_f}{W_t} \times 100 \quad (3)$$

where W_t = the total weight of drug fed, W_f = the weight of the non-encapsulated free drug.

2.6. Characterization of chitosan and Doxorubicin-loaded chitosan nanoparticles

Fourier transform infrared (FT-IR) spectrum of both CS and CS-DOX nanoparticles were taken with potassium bromide pellets on a spectrometer (JASCO FT/IR-6300, Japan) at wave number range of 500–5000 cm⁻¹ with a resolution of 4.0 cm⁻¹. The nanoparticle size distribution and zeta potential of chitosan nanoparticles was determined by dynamic light scattering (DLS) using Zetasizer Nano (Malvern Instrument Co., UK) before and after loading doxorubicin. The analysis of DLS was performed at a scattering angle of 90°, at a temperature of 25 °C using samples dispersed in de-ionized distilled water. Morphological characterizations of chitosan nanoparticles were performed by Scanning Electron Microscopy (SEM) (Seron Technology AIS 2500, India). Samples were coated by spraying gold powder to make them conductive. The chitosan nanoparticles were suspended in water by sonication for 3 min to obtain a dilute suspension. A drop of dilute suspension was deposited onto a glass slide and allowed to dry.

2.7. Drug release *in vitro*

To measure the *in vitro* release of drug, CS-DOX and PLGA/CS-DOX suspensions (containing powder with the same drug content) in 50 mL of PBS buffer were prepared. At predetermined intervals, the drug concentration was determined by measuring the absorbance at a selected wavelength $\lambda_{\text{max}} = 485$ nm on a UV-vis spectrophotometer. The data are given as mean \pm standard deviation (SD) based on the measurements of the samples from three replicates.

2.8. Mass loss kinetics

The mass loss kinetics of the implants was evaluated by measuring the weight change in PBS. The loss of scaffold weights was evaluated after cultivation as follows. The initial mass of the scaffolds was measured. Then, they were allowed to degrade by placing them in phosphate buffer solution PBS (pH 7.4) and incubated at 37 °C. At selected time intervals (1, 2, 7, 14, 21, and 30 days), the implants were removed from the solution, blotted with an absorbent tissue,

dried in a vacuum oven, and then weighed. The degradation percentage was calculated by equation 4:

$$\text{Degradation (\%)} = \frac{W_i - W_f}{W_i} \times 100 \quad (4)$$

where W_i is the initial weight of the scaffold and W_f is the final weight of scaffold at the selected time intervals.

2.9. Cells culture

Murine breast cancer cell line (4T1) was purchased from Pasteur Institute, Tehran, Iran. The cells were cultured in RPMI 1640 medium (Sigma, USA) containing 10% fetal bovine serum (FBS) (Sigma, USA) and 1% antibiotics mixture containing penicillin (Sigma, USA) and streptomycin (Sigma, USA). The cells were incubated at 37 °C in a humidified incubator in 5% CO₂ atmosphere.

2.10. Animals studies

Female BALB/c mice (age: 6–8 weeks, weight: 25 ± 2 g) were purchased from the Pasteur Institute, Tehran, Iran. The mice were acclimated for at least 1 week before the start of the study for 1 week and maintained throughout at standard conditions: 24 ± 2 °C temperature, 50 ±10% relative humidity, and 12 h light/12 h dark. All mice were fed sterilized standard mouse chow and water ad libitum. All procedures verified according to the guidelines of the Institutional Animal Care and Ethics Committee of Isfahan University of Medical Sciences.

2.11. 4T1 Breast cancer implantation

BALB/c mice were injected subcutaneously (s.c.) into the 4th abdominal mammary fat pad with 1.5 × 10⁶ cells suspended in 50 µl of PBS. Tumor sizes were measured with a digital caliper every 3 days and tumor volumes were estimated using the following tumor volume equation (5) [34].

$$\text{Tumor volume} = (\text{Tumor length}) \times (\text{Tumor width})^2 / 2 \quad (5)$$

When the tumors' volume reached 50-100 mm³, mice were divided into five groups (n=8). 1) No-treatment, 2) treated with doxorubicin (10 mg/kg/day), 3) treated with the PLGA implant, 4) treated with the PLGA/CS implant, 5) treated with the PLGA/CS-DOX implants. At no-treatment group, one incision was made at the left flank of the tumor-bearing mice and sutured without implantation of any implants. It should be mentioned that for the second and fifth treatment groups, the overall injected doxorubicin dose was approximately the same. All the operations were done under anesthesia. For anesthetizing of the mice, they were intraperitoneally injected with a Ketamine-Xylazine (KX) solution (Ketamine: 191.25 mg/kg, Xylozine: 4.25 mg/kg). To manage post-surgery pain, Ketoprofen (5 mg/kg) was administered subcutaneously until next 3 days after laser administration. If any signs of pain, wounds infection, massive necrosis and hemorrhage, diffuse metastasis were observed during any steps of the study, the mice were sacrificed by KX overdose.

2.12. Implantation of the PLGA/CS-DOX implants

The mice were completely anesthetized with the combination of ketamine and xylazine. The left flank was shaved and scrubbed with betadine. The scrub solution was wiped away from the surgical site with alcohol 70 % and covered with a sterile drape. Then, a small incision was made and the implant was embedded under sterile conditions. The skin was sutured and to manage post-surgical pain, ketoprofen (5 mg/kg) was administered subcutaneously until next 72 h. The mice were monitored daily for prolonged signs of pain, weight loss or surgical site infections.

2.13. 4T1 breast tumors' metastasis

After 35 days from the cancer cells injection, the tumor-bearing mice were sacrificed and their lungs were taken out and preserved in 10% formalin for histopathological investigations and to

evaluate the metastasis nodules. In addition, organs were fixed in 10% formalin neutral buffer solution and embedded in paraffin. In the next step, dehydration was performed and the tissues were blocked. Thin sections about 5 μm were prepared in a microtome and stained by hematoxylin and eosin. Histological photographs were obtained using a digital light microscope (Olympus, Japan).

2.14. Statistical Analysis

Statistical analysis was performed using JMP 11.0. All data were analyzed by One Way ANOVA. Statistical significance was set at $P \leq 0.05$. All experiments were performed in triplicates and the results were expressed as mean \pm SD. (not significant (ns): $P > 0.05$ *: $P \leq 0.05$, **: $P \leq 0.01$, ***: $P \leq 0.001$)

3. Results and Discussion

3.1. Characterization of PLGA microspheres (PLGA) and doxorubicin-loaded chitosan nanoparticles (CS-DOX)

Chitosan nanoparticles were prepared by the ionic interaction between the positively charged amino groups ($-\text{NH}^{+3}$) of chitosan and the negatively charged phosphate groups ($-\text{P}_3\text{O}_5^{-10}$) of TPP. The yield of chitosan nanoparticles preparation was $73 \pm 4\%$. The FT-IR spectra of CS and CS-DOX nanoparticles are shown in Figure 1A. The broadband at around 3436 cm^{-1} is attributed to $-\text{NH}_2$ and $-\text{OH}$ stretching vibration, related to extra-molecular hydrogen bonding of molecules. The absorption bands appeared at 1065 cm^{-1} , 1338 cm^{-1} , and 1638 cm^{-1} are related to the drug. The characteristic absorption bands appeared at 1657 cm^{-1} (Amide I), 1598 cm^{-1} ($-\text{NH}_2$ bending), and 1320 cm^{-1} (Amide III).

The particle size distributions of CS and CS-DOX nanoparticles were investigated as shown in Figure 1B. The average particle size of CS and CS-DOX nanoparticles were $90.76 \pm 1.83\text{ nm}$

and 105.62 ± 2.25 nm, respectively which are inconsistent with Antonioua's study [35]. In addition, the zeta potential of the CS and CS-DOX nanoparticles were $+ 20.5 \pm 1.15$ mV and $+ 18.0 \pm 1.03$ mV, respectively (Figure 1C). The positive zeta potential indicates the positive surface charge in both CS and CS-DOX nanoparticles. Many studies have reported the benefits of positive surface charge for better cancer cells uptake and tumor targeting [36, 37]. SEM micrographs of CS-DOX nanoparticles are shown in Figure 1D. The CS-DOX nanoparticles had round morphology.

[Figure 1]

In addition, the PLGA microspheres' morphology and size were investigated (Figure 2). The PLGA microspheres' size was ranged from 0.5 to 6 μm (Figure 2A). The microspheres which their size ranged from 2.5 to 5 μm exhibited the most frequencies. Also, the morphology of the PLGA microspheres were evaluated by SEM photographs (Figure 2B).

[Figure 2]

In this study, the CS-DOX nanoparticles were incorporated in the PLGA-based matrix to form biodegradable implants with efficient DOX release profile. The drug release profile of PLGA/CS-DOX implants depend on the initial drug diffusion in the chitosan nanoparticles followed by erosion of the PLGA matrix. PLGA 85:15 co-polymer is known to hydrolyze at a slower rate than PLGA co-polymers containing a lower proportion of polylactic acid such as PLGA 50:50. Therefore, the implants made of PLGA 85:15 will release the encapsulated drug at a slower rate in comparison with other PLGA co-polymers [32, 38, 39]. To find the best ratio between PLGA microspheres and CS-DOX nanoparticles for designing an implant with appropriate drug release property, various ratios (PLGA:CS-DOX, 1:1, 2:1, and 4:1) were studied (Figure 3). The drug release profiles exhibit that after initial burst drug release of the 2:1

and 4:1 PLGA/CS-DOX implants within first 30 hours, the drug release was stopped and remained in the abundance line. While, the 1:1 PLGA/CS-DOX implants exhibited sustained drug release after the burst release phase. Therefore, the 1:1 PLGA/CS-DOX implants had more favorable drug release profiles in comparison with other formulations.

[Figure 3]

3.2. Drug loading and encapsulation efficiency

Drug loading and encapsulation efficiency are very important in the drug delivery systems; it's one of the determinative parameters for evaluation of the nanocarriers efficacy. As illustrated in Table 1, drug loading content had a significant effect on the encapsulation efficiency. The results indicated that more drug loading into the chitosan nanoparticles caused a higher percentage of drug lost in the loading medium. The formulation used in PLGA/CS-DOX implants has a loading content of 22.2% and encapsulation efficiency of 79%. The chitosan nanoparticles have a strong capability to load drugs regardless of their surface charge and hydrophilicity since the drugs could be loaded into the hybrid nanoparticles due to the capillary force [40].

[Table 1]

3.3. Doxorubicin release profile

The *in vitro* release of doxorubicin from the CS-DOX and PLGA/CS-DOX is shown in Figure 4, where the profile of Dox release indicates two different phases of release. The first phase is the burst or fast release of 81% and 39% of the DOX within 36 hours for the CS-DOX and PLGA/CS-DOX, respectively. The second phase is the sustained released of DOX where approximately 97% was released for CS-DOX. The cumulative percentage of the released

doxorubicin from PLGA/CS-DOX was approximately 60% within 120 hours. The slow release of DOX from implants can significantly enhance the therapeutic efficacy [41].

[Figure 4]

3.4. Mass loss kinetics

Figure 5 illustrates the weight loss percentage of the PLGA and PLGA/CS implants in PBS (pH 7.4, 37 °C). The PLGA/CS implants exhibited higher weight loss than the PLGA implants. Therefore, incorporation of chitosan nanoparticles in the PLGA implants increase the degradation rate. The main reason for this behavior can be attributed to the hydrophilic properties of chitosan [42]. Therefore, incorporation of chitosan nanoparticles as the drug carriers in the PLGA implants can increase their biodegradation.

[Figure 5]

3.5. Assessment of the PLGA/CS-DOX implants' therapeutic effects on the 4T1 breast tumor-bearing mice

When the tumors reached 50-100 mm³, the samples were implanted in the left flank of the mice (Figure 6). As Figure 7 illustrates, although the PLGA samples were ineffective on tumors' growth, the PLGA/CS implants significantly decreased the tumors' growth. This fact can be attributed to the anti-tumor and anti-proliferative properties of the chitosan nanoparticles [43]. In addition, the PLGA/CS-DOX implants had even more significant anti-tumor effect in comparison with the injection of the same amount of doxorubicin in multiple doses (5 mg/kg/day) and PLGA/CS implants. After 20 days from implantation, the PLGA/CS and PLGA/CS-DOX implants were completely degraded without any residue. However, the PLGA implants remained at the subcutaneous space of the mice (Figure 6). Therefore, the incorporation of chitosan and CS-DOX nanoparticles to the PLGA implants increase their biodegradation in

the body environment. Chitosan as a natural biodegradable biopolymer undergoes enzymatic transformation to its basic, non-toxic components in the human and animals' body. Several enzymes are involved in the chitosan degradation. Lysozyme as a non-specific protease is the main enzyme for *in vivo* degradation of chitosan-based implants. This enzyme is present in all mammalian tissues and fluids. It targets the acetylated residues of chitosan polymer and degrades chitosan to non-toxic oligosaccharides which can be excreted or incorporated to glycosaminoglycans and glycoproteins [44-46]. Also, eight human chitinases (in the glycoside hydrolase 18 family) have been identified, three of which have shown enzymatic activity [47].

[Figure 6]

[Figure 7]

The main cause of cancer patients' death is metastasis [48]. Therefore, inhibition of cancer cells metastasis is one of the main goals of cancer treatment. In this study, 4T1 breast tumors' metastasis to the lung was evaluated at different treatment groups. As Figure 8 illustrates, the PLGA/CS-DOX implants exhibited significant inhibition of metastatic nodules' formation at lungs. Their effects were even more significant than the PLGA/CS implants and doxorubicin treatment. According to previous studies, chitosan has anti-metastatic effects and decreases cancer cells migration and metastasis [49]. Doxorubicin as a chemotherapy drug has exhibited anti-metastatic properties, too [50, 51]. Therefore, a combination of these two agents in the PLGA/CS-DOX can significantly inhibit metastasis formation at the mice lungs. Generally, not only the PLGA/CS-DOX can significantly inhibit 4T1 breast tumors' growth, but also decrease the lung metastasis (Figure 8).

[Figure 8]

To have a general view of different treatment regimens effect on the breast tumor-bearing mice. The implants effect on breast tumor-bearing mice survival was evaluated. As Figure 9 illustrates, the PLGA/CS-DOX group had more survival time in comparison with other groups (Table 2). This can be explained by more inhibition of tumors' growth and metastasis by the PLGA/CS-DOX implants in comparison with the PLGA/CS implants or doxorubicin treatment.

[Figure 9] [Table 2]

Conclusions

Drug-loaded implants have exhibited many advantages over intravenous or oral drug administration, especially for cancer treatment. Therefore, biodegradable implants have received lots of attention for controlled delivery and release of anti-cancer drugs. In the present study, doxorubicin-loaded chitosan nanoparticles were incorporated into the PLGA implants for sustained release and tumor-specific drug delivery. The PLGA/CS-DOX implants could significantly inhibit 4T1 breast tumor growth and metastasis in comparison with the same amount of doxorubicin which was injected in the multiple doses. Therefore, these implantable biodegradable devices can be an appropriate choice for replacement of multiple doses injection of doxorubicin for breast cancer treatment

Financial support

This work financially supported by the Payame Noor University, Isfahan, Iran. (Grant number: IR.PNU.1397.032)

Conflict of interests

The authors declared no potential conflicts of interest with respect to the research, authorship, and/or publication of this article.

References

- [1] T. Rana, A. Chakrabarti, M. Freeman, S. Biswas, Doxorubicin-mediated bone loss in breast cancer bone metastases is driven by an interplay between oxidative stress and induction of TGF β , PloS one 8(10) (2013) e78043.
- [2] F. Ghahremani, D. Shahbazi-Gahrouei, A. Kefayat, H. Motaghi, M.A. Mehrgardi, S.H. Javanmard, AS1411 aptamer conjugated gold nanoclusters as a targeted radiosensitizer for megavoltage radiation therapy of 4T1 breast cancer cells, RSC Advances 8(8) (2018) 4249-4258.
- [3] X. Guan, Cancer metastases: challenges and opportunities, Acta Pharmaceutica Sinica B 5(5) (2015) 402-418.
- [4] A. Müller, B. Homey, H. Soto, N. Ge, D. Catron, M.E. Buchanan, T. McClanahan, E. Murphy, W. Yuan, S.N. Wagner, Involvement of chemokine receptors in breast cancer metastasis, nature 410(6824) (2001) 50.
- [5] H. Roche, L. Vahdat, Treatment of metastatic breast cancer: second line and beyond, Annals of Oncology 22(5) (2010) 1000-1010.
- [6] C. Wang, X. Sun, K. Wang, Y. Wang, F. Yang, H. Wang, Breast cancer targeted chemotherapy based on doxorubicin-loaded bombesin peptide modified nanocarriers, Drug delivery 23(8) (2016) 2697-2702.
- [7] L. Cabeza, R. Ortiz, J.L. Arias, J. Prados, M.A.R. Martínez, J.M. Entrena, R. Luque, C. Melguizo, Enhanced antitumor activity of doxorubicin in breast cancer through the use of poly (butylcyanoacrylate) nanoparticles, International journal of nanomedicine 10 (2015) 1291.
- [8] C.F. Thorn, C. Oshiro, S. Marsh, T. Hernandez-Boussard, H. McLeod, T.E. Klein, R.B. Altman, Doxorubicin pathways: pharmacodynamics and adverse effects, Pharmacogenetics and genomics 21(7) (2011) 440.
- [9] E.L. Mayer, H.J. Burstein, Chemotherapy for metastatic breast cancer, Hematology/Oncology Clinics 21(2) (2007) 257-272.
- [10] D.S. Seah, I.V. Luis, E. Macrae, J. Sohl, G. Litsas, E.P. Winer, N.U. Lin, H.J. Burstein, Use and duration of chemotherapy in patients with metastatic breast cancer according to tumor subtype and line of therapy, Journal of the National Comprehensive Cancer Network 12(1) (2014) 71-80.
- [11] S. Mitra, U. Gaur, P. Ghosh, A.J.J.o.C.R. Maitra, Tumour targeted delivery of encapsulated dextran–doxorubicin conjugate using chitosan nanoparticles as carrier, 74(1-3) (2001) 317-323.
- [12] R. Vivek, V.N. Babu, R. Thangam, K. Subramanian, S.J.C. Kannan, S.B. Biointerfaces, pH-responsive drug delivery of chitosan nanoparticles as Tamoxifen carriers for effective anti-tumor activity in breast cancer cells, 111 (2013) 117-123.
- [13] M.J.I.j.o.b.m. Prabaharan, Chitosan-based nanoparticles for tumor-targeted drug delivery, 72 (2015) 1313-1322.
- [14] H. Zhang, F. Wu, Y. Li, X. Yang, J. Huang, T. Lv, Y. Zhang, J. Chen, H. Chen, Y.J.B.j.o.n. Gao, Chitosan-based nanoparticles for improved anticancer efficacy and bioavailability of mifepristone, 7 (2016) 1861.
- [15] Y.S. Wimardhani, D.F. Suniarti, H.J. Freisleben, S.I. Wanandi, N.C. Siregar, M.-A.J.J.o.o.s. Ikeda, Chitosan exerts anticancer activity through induction of apoptosis and cell cycle arrest in oral cancer cells, 56(2) (2014) 119-126.
- [16] M. Jiang, H. Ouyang, P. Ruan, H. Zhao, Z. Pi, S. Huang, P. Yi, M.J.A.r. Crepin, Chitosan derivatives inhibit cell proliferation and induce apoptosis in breast cancer cells, 31(4) (2011) 1321-1328.

- [17] A.O. Adisa, O.O. Lawal, A.R.J.A.J.o.H.S. Adesunkanmi, Evaluation of patients' adherence to chemotherapy for breast cancer, 15(1) (2008) 22-27.
- [18] M. Puts, H. Tu, A. Tourangeau, D. Howell, M. Fitch, E. Springall, S.J.A.o.O. Alibhai, Factors influencing adherence to cancer treatment in older adults with cancer: a systematic review, 25(3) (2013) 564-577.
- [19] J.L. Arias, Novel strategies to improve the anticancer action of 5-fluorouracil by using drug delivery systems, Molecules 13(10) (2008) 2340-2369.
- [20] B.D. Weinberg, E. Blanco, J. Gao, Polymer implants for intratumoral drug delivery and cancer therapy, Journal of pharmaceutical sciences 97(5) (2008) 1681-1702.
- [21] S. Talebian, J. Foroughi, S.J. Wade, K.L. Vine, A. Dolatshahi- Pirouz, M. Mehrali, J. Conde, G.G.J.A.M. Wallace, Biopolymers for antitumor implantable drug delivery systems: recent advances and future outlook, 30(31) (2018) 1706665.
- [22] Z. Zhang, G. Kuang, S. Zong, S. Liu, H. Xiao, X. Chen, D. Zhou, Y.J.A.M. Huang, Sandwich- Like Fibers/Sponge Composite Combining Chemotherapy and Hemostasis for Efficient Postoperative Prevention of Tumor Recurrence and Metastasis, 30(49) (2018) 1803217.
- [23] G. Kuang, Z. Zhang, S. Liu, D. Zhou, X. Lu, X. Jing, Y.J.B.s. Huang, Biphasic drug release from electrospun polyblend nanofibers for optimized local cancer treatment, 6(2) (2018) 324-331.
- [24] K.E. Uhrich, S.M. Cannizzaro, R.S. Langer, K.M. Shakesheff, Polymeric systems for controlled drug release, Chemical reviews 99(11) (1999) 3181-3198.
- [25] R.A. Jain, The manufacturing techniques of various drug loaded biodegradable poly (lactide-co-glycolide)(PLGA) devices, Biomaterials 21(23) (2000) 2475-2490.
- [26] C. Bouissou, J. Rouse, R. Price, C.J.P.r. Van der Walle, The influence of surfactant on PLGA microsphere glass transition and water sorption: remodeling the surface morphology to attenuate the burst release, 23(6) (2006) 1295-1305.
- [27] R.A.J.B. Jain, The manufacturing techniques of various drug loaded biodegradable poly (lactide-co-glycolide)(PLGA) devices, 21(23) (2000) 2475-2490.
- [28] J.E. Belz, R. Kumar, P. Baldwin, N.C. Ojo, A.S. Leal, D.B. Royce, D. Zhang, A.L. van de Ven, K.T. Liby, S. Sridhar, Sustained Release Talazoparib Implants for Localized Treatment of BRCA1-deficient Breast Cancer, Theranostics 7(17) (2017) 4340.
- [29] S.D.J.J.o.p.s. Allison, Effect of structural relaxation on the preparation and drug release behavior of poly (lactic-co-glycolic) acid microparticle drug delivery systems, 97(6) (2008) 2022-2035.
- [30] R.C. Mundargi, V.R. Babu, V. Rangaswamy, P. Patel, T.M.J.J.o.C.R. Aminabhavi, Nano/micro technologies for delivering macromolecular therapeutics using poly (D, L-lactide-co-glycolide) and its derivatives, 125(3) (2008) 193-209.
- [31] F. Mohamed, C.F.J.J.o.p.s. van der Walle, Engineering biodegradable polyester particles with specific drug targeting and drug release properties, 97(1) (2008) 71-87.
- [32] H.K. Makadia, S.J.J.P. Siegel, Poly lactic-co-glycolic acid (PLGA) as biodegradable controlled drug delivery carrier, 3(3) (2011) 1377-1397.
- [33] T.A. Ahmed, B.M.J.D.d. Aljaeid, development, therapy, Preparation, characterization, and potential application of chitosan, chitosan derivatives, and chitosan metal nanoparticles in pharmaceutical drug delivery, 10 (2016) 483.
- [34] J. Varshosaz, S. Taymouri, F. Hassanzadeh, S. Haghjooy Javanmard, M. Rostami, Folated synperonic-cholesteryl hemisuccinate polymeric micelles for the targeted delivery of docetaxel in melanoma, BioMed research international 2015 (2015).

- [35] J. Antoniou, F. Liu, H. Majeed, J. Qi, W. Yokoyama, F.J.C. Zhong, S.A. Physicochemical, E. Aspects, Physicochemical and morphological properties of size-controlled chitosan–tripolyphosphate nanoparticles, 465 (2015) 137-146.
- [36] E.J.I.j.o.n. Fröhlich, The role of surface charge in cellular uptake and cytotoxicity of medical nanoparticles, 7 (2012) 5577.
- [37] B. Yu, Y. Zhang, W. Zheng, C. Fan, T.J.I.c. Chen, Positive surface charge enhances selective cellular uptake and anticancer efficacy of selenium nanoparticles, 51(16) (2012) 8956-8963.
- [38] N. Kanthamneni, A. Chaudhary, J. Wang, S.J.I.j.o.o. Prabhu, Nanoparticulate delivery of novel drug combination regimens for the chemoprevention of colon cancer, 37(1) (2010) 177-185.
- [39] F. Chai, L. Sun, X. He, J. Li, Y. Liu, F. Xiong, L. Ge, T.J. Webster, C.J.I.j.o.n. Zheng, Doxorubicin-loaded poly (lactic-co-glycolic acid) nanoparticles coated with chitosan/alginate by layer by layer technology for antitumor applications, 12 (2017) 1791.
- [40] J.J. Wang, Z.W. Zeng, R.Z. Xiao, T. Xie, G.L. Zhou, X.R. Zhan, S.L.J.I.j.o.n. Wang, Recent advances of chitosan nanoparticles as drug carriers, 6 (2011) 765.
- [41] T. Zhang, Y. Tang, W. Zhang, S. Liu, Y. Zhao, W. Wang, J. Wang, L. Xu, K.J.J.o.M.C.B. Liu, Sustained drug release and cancer treatment by an injectable and biodegradable cyanoacrylate-based local drug delivery system, 6(8) (2018) 1216-1225.
- [42] J.R. Rodríguez-Núñez, T.J. Madera-Santana, D.I. Sánchez-Machado, J. López-Cervantes, H.S.J.J.o.P. Valdez, t. Environment, Chitosan/hydrophilic plasticizer-based films: preparation, physicochemical and antimicrobial properties, 22(1) (2014) 41-51.
- [43] L. Gibot, S. Chabaud, S. Bouhout, S. Bolduc, F.A. Auger, V.J. Moulin, Anticancer properties of chitosan on human melanoma are cell line dependent, International journal of biological macromolecules 72 (2015) 370-379.
- [44] K. Kurita, Y. Kaji, T. Mori, Y.J.C.P. Nishiyama, Enzymatic degradation of β -chitin: susceptibility and the influence of deacetylation, 42(1) (2000) 19-21.
- [45] E. Szymańska, K.J.M.d. Winnicka, Stability of chitosan—a challenge for pharmaceutical and biomedical applications, 13(4) (2015) 1819-1846.
- [46] K.M. Vårum, M.M. Myhr, R.J. Hjerde, O.J.C.r. Smidsrød, In vitro degradation rates of partially N-acetylated chitosans in human serum, 299(1-2) (1997) 99-101.
- [47] J.D. Funkhouser, N.N.J.B.e.b. Aronson, Chitinase family GH18: evolutionary insights from the genomic history of a diverse protein family, 7(1) (2007) 96.
- [48] T.N. Seyfried, L.C.J.C.r.i.o. Huysentruyt, On the origin of cancer metastasis, 18(1-2) (2013) 43.
- [49] P.D. Potdar, A.U.J.J.o.C.M. Shetti, T. Volume, Evaluation of anti-metastatic effect of chitosan nanoparticles on esophageal cancer-associated fibroblasts, 2 (2016) 260.
- [50] L.E. Aguilar, R.G. Thomas, M.J. Moon, Y.Y. Jeong, C.H. Park, C.S.J.E.J.o.P. Kim, Biopharmaceutics, Implantable chemothermal brachytherapy seeds: A synergistic approach to brachytherapy using polymeric dual drug delivery and hyperthermia for malignant solid tumor ablation, 129 (2018) 191-203.
- [51] E.M. Mastria, M. Chen, J.R. McDaniel, X. Li, J. Hyun, M.W. Dewhirst, A.J.J.o.c.r. Chilkoti, Doxorubicin-conjugated polypeptide nanoparticles inhibit metastasis in two murine models of carcinoma, 208 (2015) 52-58.

Figure legends:

Figure 1: Characterization of the chitosan nanoparticles (CS) and doxorubicin-loaded chitosan nanoparticles (CS-DOX). (A) FT-IR spectra of the CS and CS-DOX nanoparticles. (B) Size distribution and (C) zeta potential of the CS and CS-DOX nanoparticles. (D) SEM micrographs of the CS-DOX nanoparticles.

Figure 2: Characterization of the PLGA microspheres. (A) Sizes distribution and (B) SEM micrographs of the PLGA microspheres.

Figure 3: Doxorubicin release profiles of PLGA/CS-DOX implants with different formulations (1:1, 2:1, 4:1).

Figure 4: Doxorubicin release profiles of the CS-DOX and PLGA/CS-DOX implants in PBS.

Figure 5: Mass loss kinetics of the PLGA and PLGA/CS implants in PBS.

Figure 6: Photograph of different implants including (A) PLGA, (B) PLGA/CS, and (C) PLGA/CS-DOX implants. (D-G) Implantation of the samples at the left flank of the tumor-bearing mice. The photographs from left to right illustrate the implantation procedure step by step ,including (D) anesthetizing the mice, (E) making a small incision, (F) subcutaneous implantation of the PLGA/CS-DOX in the incision site, and (G) suturing of the incision. (H-J) Photographs exhibit the biodegradation efficacy of (H) the PLGA, (I) the PLGA/CS, (J) and the PLGA/CS-DOX implants 20 days after the implantation. The PLGA/CS and PLGA/CS-DOX implants were completely degraded, but the PLGA implants maintained their structure which was engulfed by the surrounding tissues. No-sign of skin damage was observed.

Figure 7: Therapeutic effect of the implants on the 4T1 breast tumors' growth in the tumor-bearing mice (n=8). The PLGA/CS-DOX implants exhibited the most anti-tumor effect. (not significant (ns): $P > 0.05$ *: $P \leq 0.05$, **: $P \leq 0.01$, ***: $P \leq 0.001$)

Figure 8: The implants effects on the metastatic nodules' formation at the lungs of tumor-bearing mice (n=5). (not significant (ns): $P > 0.05$ *: $P \leq 0.05$, **: $P \leq 0.01$, ***: $P \leq 0.001$)

Figure 9: The tumor-bearing mice survival time at different treatment groups (n=8). The PLGA/CS-DOX implants could significantly increase the breast tumor-bearing mice survival time. (not significant (ns): $P > 0.05$ *: $P \leq 0.05$, **: $P \leq 0.01$, ***: $P \leq 0.001$)

Table 1: Drug loading concentration, loading content, and encapsulation efficiency

Samples	Weight of chitosan (mg)	Weight of PLGA (mg)	Weight of drug (mg)	Loading content (%)	Encapsulation efficiency (%)
PLGA	---	50	---	---	---
PLGA/CS	25	25	---	---	---
PLGA/CS-DOX	22.5	22.5	5	22.2	79

Table 2: Mean survival time of the tumor-bearing mice in different treatment groups.

Groups	Mean survival time (Days)
No-treatment (n=8)	51 ± 8.5
PLGA (n=8)	53.5 ± 9.8
PLGA/CS (n=8)	71.1 ± 10
PLGA/CS-DOX (n=8)	94 ± 12.3 *
Doxorubicin (n=8)	76 ± 11.6

*: P ≤ 0.05, n: the number of mice in each group.

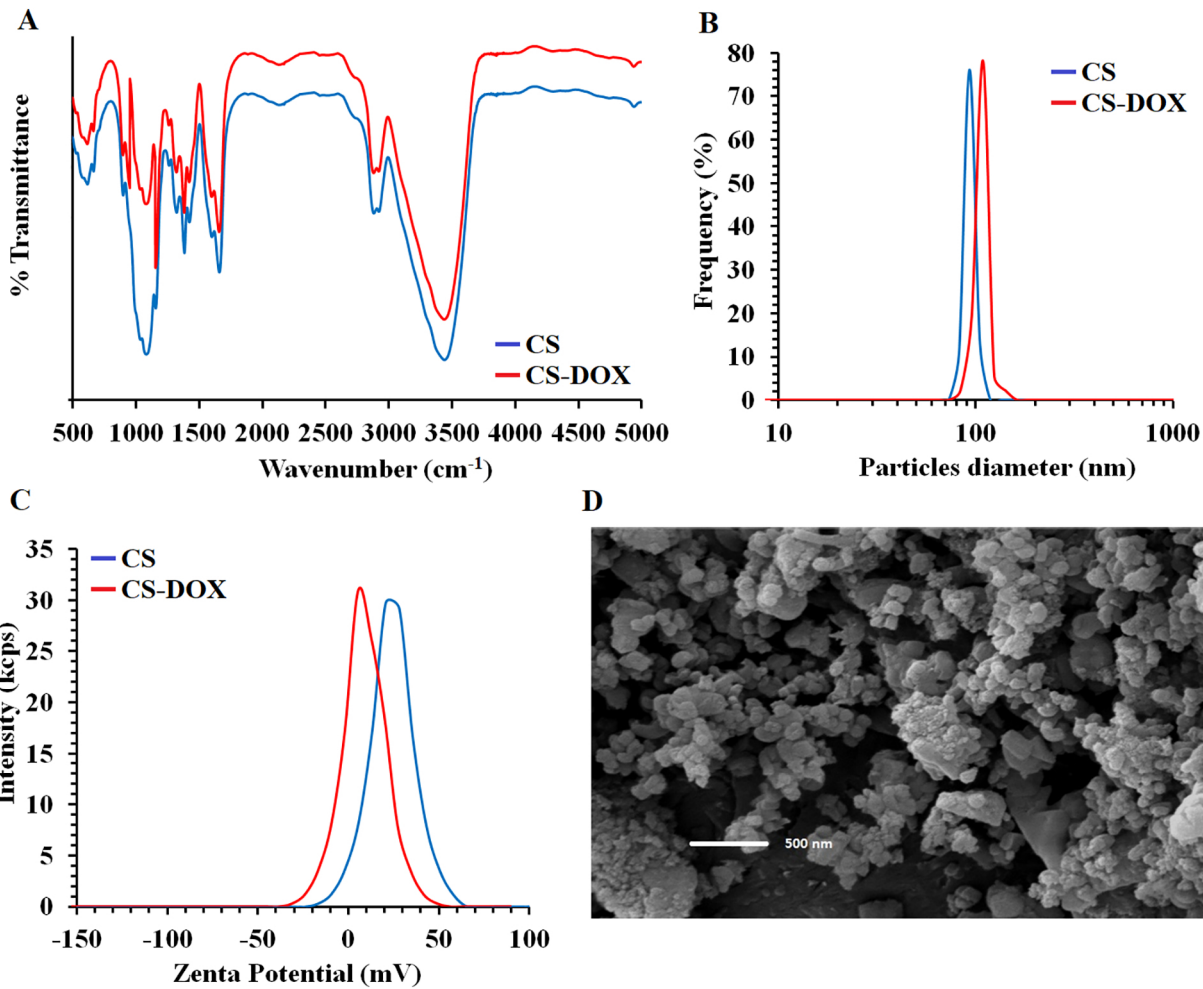


Figure 1

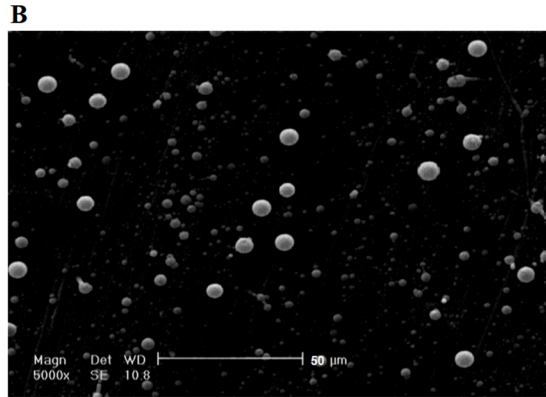
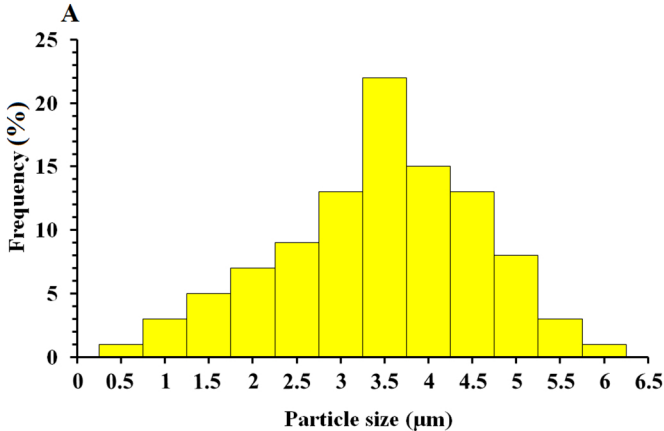


Figure 2

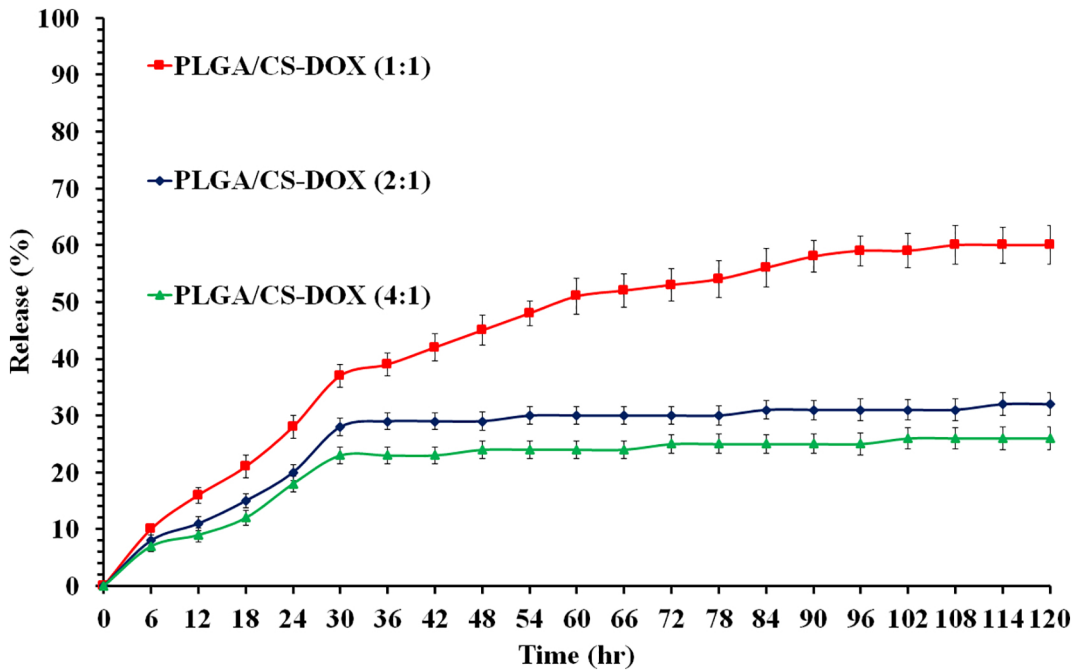


Figure 3

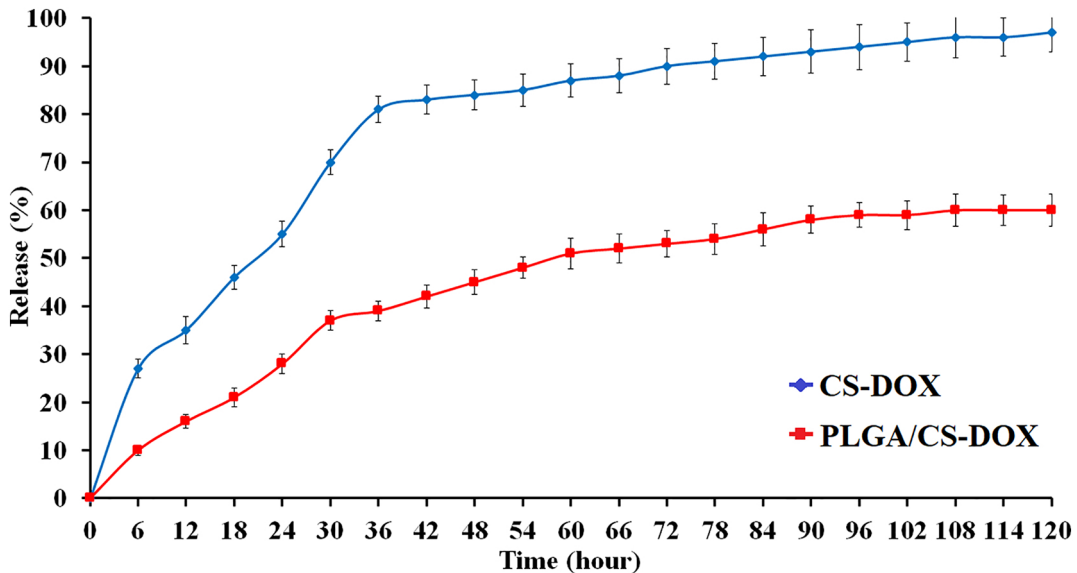


Figure 4

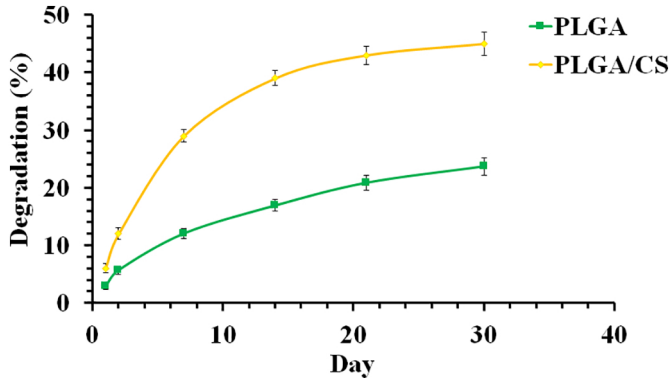


Figure 5

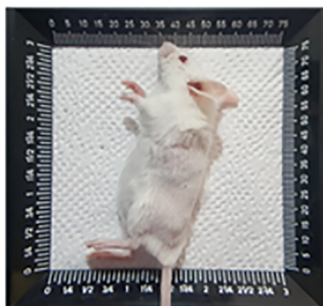
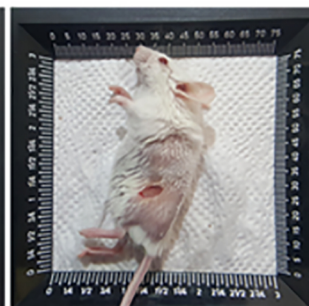
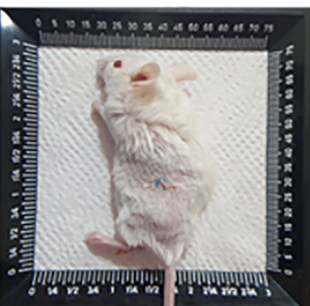
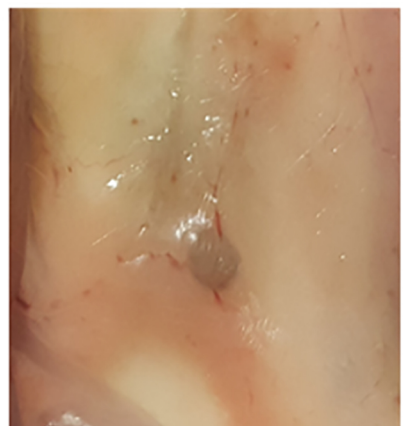
A**B****C****D****E****F****G****H****I****J**

Figure 6

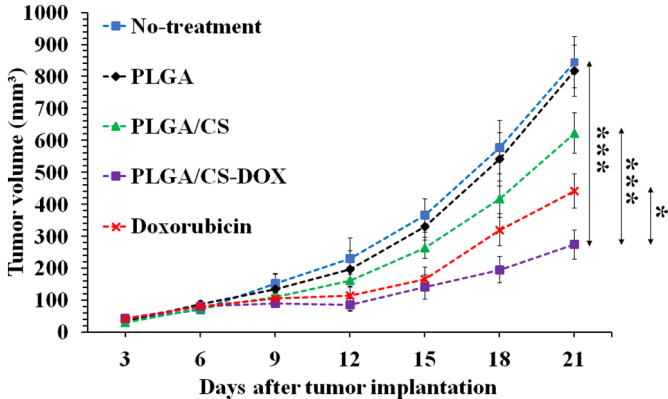


Figure 7

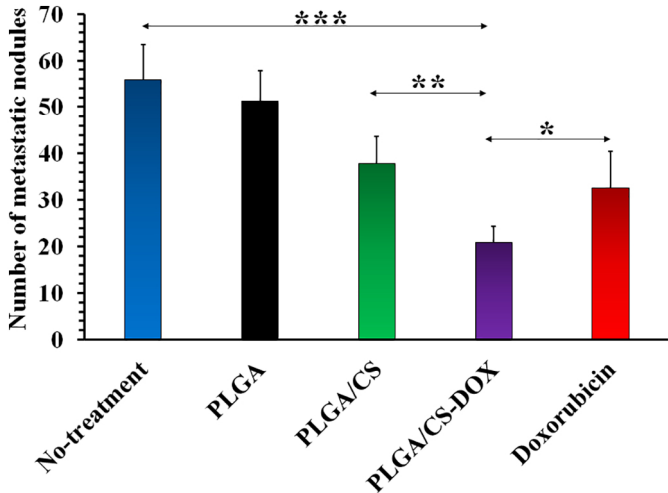


Figure 8

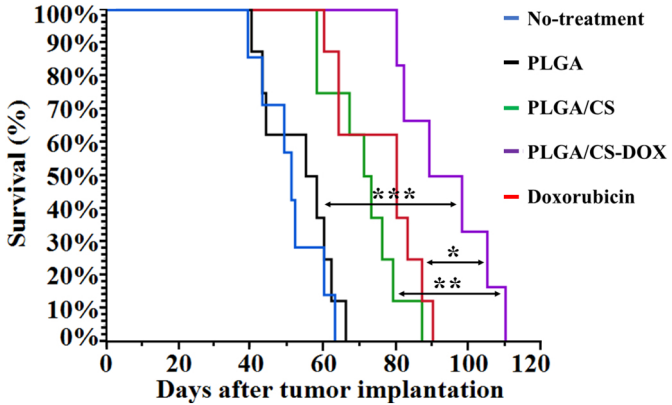


Figure 9